Bioorganic Chemistry

ISSN 1993-6842 (on-line); ISSN 0233-7657 (print)
Biopolymers and Cell. 2016. Vol. 32. N 4. P 289–299
doi: http://dx.doi.org/10.7124/bc.00092B

UDC 577.336+667.287.4

Design of 4-(4-dialkylaminostyryl) -pyridinium dyes for fluorescent detection of amyloid fibrils

D. I. Inshyn, S. V. Chernii, V. B. Kovalska, S. M. Yarmoluk

Institute of Molecular Biology and Genetics, NAS of Ukraine
150, Akademika Zabolotnoho Str., Kyiv, Ukraine, 03680
d.i.inshyn@imbg.org.ua

The pathological proteins aggregation into the fibrillar structures is common to a large group of amyloid-related disorders, such as neurodegenerative diseases. Accordingly, there is a need for development of analytical tools, particularly fluorescent probes for detection of amyloid fibrils. **Aim.** To design amyloid-sensitive styrylpyridinium fluorescent dyes. **Methods.** QSAR model for the prediction of the dye efficiency followed by the synthesis and spectral-luminescent studies. **Results.** Nine structures with the highest predicted efficiency were selected from the virtual database of 1500 styrylcyanines; these compounds were synthesized and their spectral-luminescent properties in the presence of amyloidogenic protein insulin were studied. The dyes are weakly fluorescent when free and have a low sensitivity to native insulin. In the presence of insulin fibrils, they increase the fluorescence intensity up to dozens of times depending on the nature of the terminal substituent. The dye with a *4-methylpiperidinyl* substituent demonstrated the highest fluorescence response (up to 23 times) and a wide range of fibril detection (1–40 μg/ml). **Conclusion.** (4-(4-dialkylaminostyryl) -pyridinium dyes with cyclic aliphatic terminal substituent have the properties of fluorescent probes for sensing the amyloid fibrils. The prediction accuracy of the regression model is suitable for the majority of the styrylcyanines but poor in the case of the dyes with piperazinyl substituent or those containing additional aromatic substituents.

Keywords: fluorescent probes, styrylcyanine dyes, synthesis, regression model QSAR, amyloid fibrils, protein detection

Introduction

A pathological self-assembly of proteins into the insoluble fibrillar aggregates is common to a large group of amyloid-related disorders, such as neurodegenerative diseases, amyloidosis, prion diseases and type II diabetes [1–3]. A protein involved in the amyloid fibrils is specific to each disease. Despite of the fact that various amyloidogenic proteins do not reveal any simple amino acids sequence homology, all amyloid formations possess similar structural and morphological properties [4].

Among fast and convenient methods of the detection of the amyloid fibrils and study of their formation is the usage of fluorescent probes that are sensitive to their beta-pleated structure. The benzothiazole dye Thioflavin T and its derivatives are mostly used in this application [5]. Recently mono- and trimethine cyanine dyes were developed as efficient fluorescent probes that were able to discriminate the amyloid aggregates [6, 7]. Additionally, the fluorescent sensitivity of beta-ketoenoles to the fibrillar aggregates has been recently discovered [8]. However, there is still a request for the design of new fluorescent molecules with high selectivity to the amyloid formations.

It is suggested that fluorescence of dye molecules increases due to their rigid fixation in the rows formed

by the beta pleats of polypeptide chains (binding channels). This way the dye molecules possess fluorescent sensitivity to a structural motif common for the amyloid aggregates formed by various proteins.

Recently we for the first time have applied a QSAR method as a part of ligand based virtual screening to design fluorescent dyes that are sensitive to the amyloid fibrils [9]. The artificial neural network (ANN) methodology was evaluated to build the regression model of activity prediction. The most influential descriptors chosen for the developing of this model are connected with the structural parameters of the dye molecule and thus reflected its complementarity to the structure of the binding channel of the amyloid fibril. The developed model was able to predict a fluorescent response of the cyanine dyes to the fibrils of alpha synuclein (ASN). In the present work we apply this regression model to design the amyloid-sensitive dyes based on the styrylpyridinium fragment, the molecules of this kind were earlier shown as fluorescent reporters for DNA and fibrillar aggregates [10]. The elongated shape of styrylpyridinium molecule provides a good fitting to the grooves formed either by double strands of DNA or by the beta pleats of amyloid fibril. As a model for the current studies, the amyloidogenic protein insulin is used. The morphology of its protofilaments distincts from that of ASN (native protein contains one polypeptide chain) since insulin consists of two polypeptide chains, that remain bounded during the fibril formation. The polypeptide chain A of insulin is placed out of fibrilar core and thus distored the geometry of the binding channel [11].

The regression model applied on the virtual database of about 1500 styrylcyanines to predict the fluorescent sensitivity of about 120 compounds to amyloid fibrils. The nine of these styrylcyanine dyes with a variation of terminal substituents are synthesized. The fluorescent properties of these dyes when free and in the presence of native and fibrillar insulin are studied, the linear range of fibril detection provided by the dyes is determined. The accuracy of the prediction provided by the earlier developed regression model and thus its versatility is estimated.

Materials and Methods

Data sets and processing. All manipulations with structures were done in InstantJChem suite (InstantJChem, ver. 14.12.15.0, 2014, ChemAxon, http://www.chemaxon.com). The virtual database of compounds was created using cross-linking of reagents based on the chemical classes of known amyloid-sensitive dyes [5]. All compounds were considered only *trans*- isomers. The structures were prepared by error checking, subsequent 2D cleaning and geometrical optimization.

Molecular descriptors calculation. Molecular descriptors were calculated using the InstantJChem. This program calculates descriptors of six categories: constitutional descriptors, electronic descriptors, physicochemical properties, topological indices, geometrical molecular descriptors, and quantum chemistry descriptors.

Regression model evaluation. As for other data, their processing and regression analysis was carried out with the same method as that described in our previous work [9].

General methods. Melting points were determined in capillaries by heating with a heating gun and were not corrected. Chromatographic separations were performed on silica gel 60 (40–6.3 mm) with analytical grade solvents, driven by a positive pressure of air; Rf values refer to TLC (visualized with UV light) carried out on alumina backed plates coated with 25 mm silica gel (Merck F_{254}), with the same eluant indicated for the column chromatography. The solvent removal was performed by evaporation on a rotavap at 40 °C. The 1H NMR spectra were recorded with a Varian Mercury VXR 400 spectrometer (operating at 400 MHz for 1H). The 1H NMR data are reported as multiplicity (s = singlet, d = doublet, t = triplet, q = quartet, m = multiplet or unresolved, br = broad signal), coupling constant(s) in Hz, integration). The chemical shifts were determined relative to the residual solvent peak ($CHCl_3$: d=7.27 ppm for 1H NMR; DMSO-d_6: d = 2.49 ppm). Dimethylformamide (DMF), n-butyl alcohol, isopropyl alcohol (IPA), methyl tert-butyl ether (MTBE) were purchased from MacroChem (Kyiv) and distilled. All other reagents

were purchased from Acros Organics (BE) unless otherwise stated.

Synthesis of compounds. *1, 4-dimethylpyridin-1-ium iodide*: a solution of 4-picoline 18.6 g (200 mmol) in $CHCl_3$ 100 ml was treated with methyl iodide 57.4 g (31.5 ml, 500 mmol, 2.5 eq.). Reaction mixture was left to stand for 4 days and crystalline solid was separated by filtration and washed with MTBE for 3 times. Yield 36.4 g, 77.5%.

Typical procedure for obtaining the substituted aldehydes: a solution of 6.21 g (50 mmol) of 4-fluorobenzaldehyde in 30 ml of DMF under argon was treated with the appropriate secondary amine (60 mmol) and anhydrous potassium carbonate 17.27 g (125 mmol, 2.5 eq.) at 110 °C for 16–24 hours. The end of the reaction was monitored on TLC. Reaction mixture was poured into the water 200 ml and extracted with MTBE 3 times. Organic extracts were washed with water and brine, dried on Na_2SO_4 and evaporated. Compounds were subjected to chromatographic purification on SiO_2 with Hexane/Ethyl acetate. Compounds were stored under argon.

4-(piperidin-1-yl)benzaldehyde, Ia. Yield 62%, m.p. 76–78 °C. 1H NMR ($CDCl_3$): 1.69 (br s, 6H, CH_2CH_2CH_2), 3.39 (br s, 4H, CH_2NCH_2), 6.86 (d, J = 7.7 Hz, 2H, C$H_{arom.}$), 7.67 (d, J = 7.7 Hz, 2H, C$H_{arom.}$), 9.72 (s, 1H, C*H*O).

4-(azepan-1-yl)benzaldehyde, Ib. Yield 75%, oil. 1H NMR ($CDCl_3$): 1.56 (br s, 4H, CH_2CH_2), 1.81 (br s, 4H, NCH$_2$CH_2), 3.53 (br s, 4H, CH_2NCH_2), 6.64 (d, J = 8.6 Hz, 2H, C$H_{arom.}$), 7.62 (d, J = 8.6 Hz, 2H, C$H_{arom.}$), 9.65 (s, 1H, C*H*O).

4-(morpholin-4-yl)benzaldehyde, Ic. Yield 67%, m.p. 82–84 °C. 1H NMR ($CDCl_3$): 3.29 (t, J = 4.5 Hz, 4H, CH_2NCH_2), 3.79 (t, J = 4.1 Hz, 4H, CH_2OCH_2), 6.86 (d, J = 8.5 Hz, 2H, C$H_{arom.}$), 7.68 (d, J = 8.5 Hz, 2H, C$H_{arom.}$), 9.74 (s, 1H, C*H*O).

4-(4-methylpiperidin-1-yl)benzaldehyde, Id. Yield 62%, oil. 1H NMR ($CDCl_3$): 0.98 (d, J = 6.2 Hz, 3H, CH_3), 1.23 – 1.35 (m, 2H, CH_2CHCH_2), 1.55 – 1.68 (m, 1H, CH$_3$C*H*), 1.73 (d, J = 12.7, 2H, CH_2CHCH_2), 2.88 (t, J = 12.4 Hz, 2H, CH_2NCH_2), 3. 88 (d, J = 10.9 Hz, 2H, CH_2NCH_2), 6.83 (d, J = 7.4 Hz, 2H, C$H_{arom.}$), 7.64 d, 2H, J = 7.4 Hz, C$H_{arom.}$), 9.69 (s, 1H, C*H*O).

4-(4-methylpiperazin-1-yl)benzaldehyde, Ie. Yield 54%, m.p. 44–47 °C. 1H NMR ($CDCl_3$): 2.24 (s, 3H, CH_3), 2.32 (t, J = 4.5 Hz, 4H, CH_2N(CH$_3$)CH_2), 3.29 (t, J = 4.5 Hz, 4H, CH_2N$_{Ar.}$CH_2), 6.79 (d, J = 8.4 Hz, 2H, C$H_{arom.}$), 7.61 (d, J = 6.4 Hz, 2H, CH_{arom}), 9.67 (s, 1H, C*H*O).

4-(3-methylpiperidin-1-yl)benzaldehyde, If. Yield 52%, yellow oil 1H NMR ($CDCl_3$): 0.96 (d, J = 6.4 Hz, 3H, CH_3), 1.07 – 1.19 (m, 1H, C*H*), 1.61 – 1.89 (m, 4H, CH_2 + CH_2), 2.52 (t, J = 10.7 Hz, 1H, NCH_2), 2.84 (t, J = 12.3 Hz, 1H, NCH_2), 3.79 (dd, J = 19.8, 8.5 Hz, 2H, NCH_2), 6.82 (d, J = 8.3 Hz, 2H, C$H_{arom.}$), 7.62 (d, J = 8.3 Hz, 2H, C$H_{arom.}$), 9.68 (s, 1H, C*H*O).

Tert-butyl 4-(4-formylphenyl) piperazine-1-carboxylate, I g. Yield 50%. 1H NMR ($CDCl_3$): 1.47 (s, 9H, t-Bu), 3.34 (br s, 4H, CH_2NCH_2), 3.56 (br s, 4H, CH_2NCH_2), 6.86 (d, J = 8.4 Hz, 2H, C$H_{arom.}$), 7.69 (d, J = 8.7 Hz, 2H, C$H_{arom.}$), 9.75 (s, 1H, C*H*O).

4-(4-phenylpiperazin-1-yl)benzaldehyde, Ij. Yield 72%, m.p. 93–95 °C. 1H NMR ($CDCl_3$): 3.32 (br s, 4H, CH_2NCH_2), 3.56 (br s, 4H, CH_2NCH_2), 6.79 (t, J = 6.9 Hz, 1H, C$H_{arom.}$), 6.94 (d, J = 7.8 Hz, 2H, C$H_{arom.}$), 7.04 (d, J = 8.4 Hz, 2H, C$H_{arom.}$), 7.21 (t, J = 7.1 Hz, 2H, C$H_{arom.}$), 7.71 (d, J = 8.6 Hz, 2H, C$H_{arom.}$), 9.71 (s, 1H, C*H*O).

4-(4-benzylpiperidin-1-yl)benzaldehyde, Ih. Yield 64%, m.p. 77–79 °C. 1H NMR ($CDCl_3$): 1.22 – 1.37 (m, 2H, CH_2CHCH_2), 1.62 – 1.80 (m, 3H, CH_2 + C*H*(Bn)), 2.51 (d, J = 6.9 Hz, 2H, BnCH_2), 2.81 (t, J = 12.1 Hz, 2H, CH_2NCH_2), 3.86 (d, J = 12.5 Hz, 2H, CH_2NCH_2), 6.79 (d, J = 8.3 Hz, 2H, C$H_{arom.}$), 7.05 (t, J = 7.5, 2H, C$H_{arom.}$), 7.12 (t, J = 7.4, 1H, C$H_{arom.}$), 7.17 – 7.24 (m, 2H, C$H_{arom.}$), 7.62 (d, J = 8.3 Hz, 2H, C$H_{arom.}$), 9.67 (s, 1H, C*H*O).

General procedure for preparation of styryl compounds*:* a solution of 1, 4-dimethylpyridin-1-ium iodide 0.235 mg (1 mmol) and appropriate aldehyde (1.1 mmol, 1.1 eq.) in 5ml of n-butanol was heated at 140 °C in oil bath with stirring for 6 hours. Crystals were collected, filtered and washed with IPA. Compounds were recrystallized from a mixture of IPA and DMF.

1-methyl-4-[(E)-2-[4-(piperidin-1-yl)phenyl] ethenyl]pyridin-1-ium iodide, IIa. Yield 41%. M.p. 202 °C. 1H NMR (DMSO-d_6): 1.66 (br s, 6H, $CH_2CH_2CH_2$), 3.63 (br s, 4H, CH_2NCH_2), 4.25 (s, 3H, CH_3), 6.92 (d, J = 7.2 Hz, 2H, $CH_{arom.}$), 7.14 (d, J = 16.0 Hz, 1H, $CH_{vinyl.}$), 7.56 (d, J = 7.2 Hz, 2H, $CH_{arom.}$), 7.85 (d, J = 16.0 Hz, 1H, $CH_{vinyl.}$), 8.07 (d, J = 4.3 Hz, 2H, $CH_{Py.}$), 8.74 (d, J = 4.3 Hz, 2H, $CH_{Py.}$).

4-[(E)-2-[4-(azepan-1-yl)phenyl]ethenyl]-1-methylpyridin-1-ium iodide, IIb. Yield 40%. M.p. 158 °C. 1H NMR (DMSO-d_6): 1.55 (br s, 4H, CH_2CH_2), 1.80 (br s, 4H, NCH_2CH_2), 3.56 (t, J = 12.0 Hz, 4H, CH_2NCH_2), 4.24 (s, 3H, CH_3), 6.72 (d, J = 8.2 Hz, 2H, $CH_{arom.}$), 7.05 (d, J = 16.3 Hz, 1H, $CH_{vinyl.}$), 7.55 (d, J = 8.2 Hz, 2H, $CH_{arom.}$), 7.84 (d, J = 16.3 Hz, 1H, $CH_{vinyl.}$), 8.01 (d, J = 6.0 Hz, 2H, $CH_{Py.}$), 8.72 (d, J = 6.0 Hz, 2H, $CH_{Py.}$).

1-methyl-4-[(E)-2-[4-(morpholin-4-yl)phenyl] ethenyl]pyridin-1-ium iodide, IIc. Yield 57%. M.p. 188 °C. 1H NMR (DMSO-d_6): 3.00 (s, 3H, CH_3), 3.28 (br s, 4H, CH_2NCH_2), 3.79 (br s, 4H, CH_2OCH_2), 4.28 (s, 3H, CH_3), 6.72 (d, J = 8.5 Hz, 2H, $CH_{arom.}$), 7.21 (d, J = 16.2 Hz, 1H, $CH_{vinyl.}$), 7.61 (d, J = 8.2 Hz, 2H, $CH_{arom.}$), 7.88 (d, J = 16.3 Hz, 1H, $CH_{vinyl.}$), 8.10 (d, J = 6.1 Hz, 2H, $CH_{Py.}$), 8.79 (d, J = 6.1 Hz, 2H, $CH_{Py.}$).

1-methyl-4-[(E)-2-[4-(4-methylpiperidin-1-yl) phenyl]ethenyl]pyridin-1-ium iodide, IId. Yield 46%. M.p. 217 °C. 1H NMR (DMSO-d_6): 0.99 (d, J = 6.2 Hz, 3H, CH_3), 1.19 – 1.31 (m, 2H, CH_2CHCH_2), 1.56 – 1.68 (m, 1H, CH_3CH), 1.75 (d, J = 12.1 Hz, 2H, CH_2CHCH_2), 2.85 (t, J = 11.5 Hz, 2H, CH_2NCH_2), 3.89 (d, J = 12.2 Hz, 2H, CH_2NCH_2), 4.24 (s, 3H, CH_3), 6.91 (d, J = 8.1 Hz, 2H, $CH_{arom.}$), 7.14 (d, J = 16.1 Hz, 1H, $CH_{vinyl.}$), 7.55 (d, J = 8.1 Hz, 2H, $CH_{arom.}$), 7.85 (d, J = 16.1 Hz, 1H, $CH_{vinyl.}$), 8.05 (d, J = 6.0 Hz, 2H, $CH_{Py.}$), 8.75 (d, J = 6.0 Hz, 2H, $CH_{Py.}$).

1-methyl-4-[(E)-2-[4-(4-methylpiperazin-1-yl) phenyl]ethenyl]pyridin-1-ium iodide, IIe. Yield 27%. M.p. 196 °C. 1H NMR (DMSO-d_6): 2.26 (s, 3H, CH_3), 3.07 (br s, 4H, $CH_2N(CH_3)CH_2$), 3.32 (br s, 4H, $CH_2N_{Ar.}CH_2$), 4.25 (s, 3H, CH_3), 6.93 (d, J = 8.0 Hz, 2H, $CH_{arom.}$), 7.18 (d, J = 16.0 Hz, 1H, $CH_{vinyl.}$), 7.59 (d, J = 8.0 Hz, 2H, $CH_{arom.}$), 7.65 (d, J = 16.0 Hz, 1H, $CH_{vinyl.}$), 8.07 (d, J = 5.6 Hz, 2H, $CH_{Py.}$), 8.75 (d, J = 5.6 Hz, 2H, $CH_{Py.}$).

1-methyl-4-[(E)-2-[4-(3-methylpiperidin-1-yl) phenyl]ethenyl]pyridin-1-ium iodide, IIf. Yield 46%. M.p. 162 °C. 1H NMR (DMSO-d_6): 0.97 (d, J = 6.2 Hz, 3H, CH_3), 1.09 – 1.21 (m, 1H, CH), 1.57 – 1.89 (m, 4H, $CH_2 + CH_2$), 2.49 (br s, 1H, NCH_2), 2.82 (t, J = 12.1 Hz, 1H, NCH_2), 3.81 (t, J = 6.5 Hz, 2H, NCH_2), 4.26 (s, 3H, CH_3), 6.93 (d, J = 8.2 Hz, 2H, $CH_{arom.}$), 7.15 (d, J = 16 Hz, 1H, $CH_{vinyl.}$), 7.55 (d, J = 8.2 Hz, 2H, $CH_{arom.}$), 7.86 (d, J = 16.0 Hz, 1H, $CH_{vinyl.}$), 8.07 (d, J = 5.9 Hz, 2H, $CH_{Py.}$), 8.77 (d, J = 5.9 Hz, 2H, $CH_{Py.}$).

4-[(E)-2-(4-{4-[(tert-butoxy)carbonyl]piperazin-1-yl]phenyl)ethenyl]-1-methylpyridin-1-ium, IIg. Yield 34%. 1H NMR (DMSO-d_6): 1.45 (s, 9H, t-Bu), 3.32 (br s, 4H, CH_2NCH_2), 3.51 (br s, 4H, CH_2NCH_2), 4.25 (s, 3H, CH_3), 6.96 (d, J = 8.1 Hz, 2H, $CH_{arom.}$), 7.20 (d, J = 16.1 Hz, 1H, $CH_{vinyl.}$), 7.59 (d, J = 8.1 Hz, 2H, $CH_{arom.}$), 7.89 (d, J = 16.1 Hz, 1H, $CH_{vinyl.}$), 8.11 (d, J = 5.5 Hz, 2H, $CH_{Py.}$), 8.77 (d, J = 5.5 Hz, 2H, $CH_{Py.}$).

1-methyl-4-[(E)-2-[4-(4-phenylpiperazin-1-yl] ethenyl]pyridin-1-ium iodide, IIj. Yield 43%. M.p. 179 °C. 1H NMR (DMSO-d_6): 3.32 (br s, 4H, CH_2NCH_2), 3.50 (br s, 4H, CH_2NCH_2), 4.27 (s, 3H, CH_3), 6.79 (t, J = 7.1 Hz, 1H, $CH_{arom.}$), 6.94 (d, J = 7.8 Hz, 2H, $CH_{arom.}$), 7.02 (d, J = 8.3 Hz, 2H, $CH_{arom.}$), 7.14 – 7.28 (m, 3H, $CH_{arom.} + CH_{vinyl.}$), 7.62 (d, J = 8.2 Hz, 2H, $CH_{arom.}$), 7.89 (d, 1H, J = 16.2, 1H, $CH_{vinyl.}$), 8.09 (d, J = 5.1 Hz, 2H, $CH_{Py.}$), 8.78 (d, J = 5.1 Hz, 2H, $CH_{Py.}$).

4-[(E)-2-[4-(4-benzylpiperidin-1-yl)phenyl] ethenyl]-1-methylpyridin-1-ium iodide, IIh. Yield 37%. M.p. 173 °C. 1H NMR (DMSO-d_6): 1.23 – 1.37 (m, 2H, $CH_2CH(Bn)CH_2$), 1,65 – 1.83 (m, 3H, $CH_2 + CH(Bn)$), 2.56 (br s, 2H, $PhCH_2$), 2.81 (t, J = 12.0 Hz, 2H, CH_2NCH_2), 3.87 (d, J = 12.0 Hz, 2H, CH_2NCH_2), 4.26 (s, 3H, CH_3), 6.90 (d, J = 7.3 Hz, 2H, $CH_{arom.}$), 7.10 – 7.18 (m, 4H, $CH_{arom.}$), 7.21 – 7.27 (m, 2H, $CH_{arom.} + CH_{vinyl.}$), 7.56 (d, J = 7.7 Hz, 2H, $CH_{arom.}$), 7.85 (d, J = 16 Hz, 1H, $CH_{vinyl.}$), 8.06

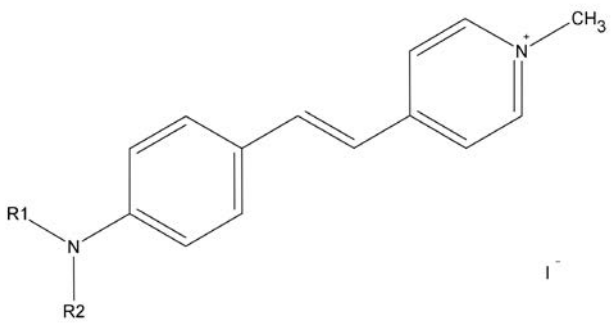

Fig. 1. Base scaffold of styrylpyridines, the NR1R2 substituents are presented in the Table 1.

(d, J = 5.0 Hz, 2H, C$H_{Py.}$), 8.77 (d, J = 5.1 Hz, 2H, C$H_{Py.}$).

Preparation of solutions. The dyes stock solutions were prepared by dissolving the dyes at 2 mM concentration in DMF. Working solutions of free dyes were prepared by diluting stock solutions in 50 mM Tris-HCl buffer (pH 7.9) to the concentration 2 μM. The working solutions of dye-proteins complexes were prepared by adding the aliquot of stock solution of monomer insulin or fibrillar insulin aggregates to the 2 μM dye solution, insulin concentration in the working solution was 3.4 μM. The insulin stock solution was prepared by dissolving 0.1 mM HCl water solution to 2 mg/ml concentration.

Insulin fibril formation. Human insulin (Sigma-Aldrich) was dissolved at 340 μM (2 mg/ml) concentration in 0.1 mM water solution of HCl (pH = 2). The amyloid fibrils were formed by incubating the protein solution in a Thermomixer incubator at 65 °C for about 5 h. The presence of fibrillar insulin aggregates was confirmed by the atomic force microscopy.

Spectral properties of free dyes and of dyes in the presence of insulin. The fluorescence spectra were registered using the fluorescent spectrophotometer Cary Eclipse (Varian, Australia).The absorption was registered using the spectrophotometer Specord M – 40 (Germany, Carl Zeiss).The fluorescence emission was excited on the wavelength of the corresponding excitation maxima. The experiments were performed at room temperature.

Fluorescence quantum yields recording. The evaluation of dyes quantum yields was carried out

Table 1. **Substituents in a set of the synthesized dyes.**

Number	Name of NR_1R_2 group	Structure of NR_1R_2 group
IIa	piperidin-1-yl-	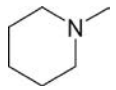
IIb	azepan-1-yl-	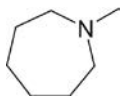
IIc	morpholin-4-yl-	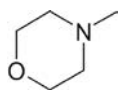
IId	4-methylpiperidin-1-yl-	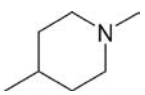
IIe	4-methylpiperazin-1-yl-	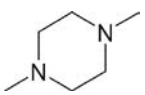
IIf	3-methylpiperidin-1-yl-	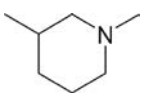
IIg	4-[(tert-butoxy)carbonyl] piperazin-1-yl group	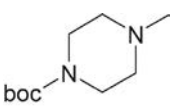
IIj	4-phenylpiperazin-1-yl-	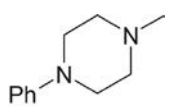
IIh	4-benzylpiperidin-1-yl-	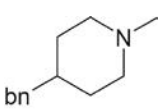

by the comparative method which involved the use of well characterized standard sample (Rhodamine 6G) with known Φ_F value (0.95) [12, 13]. The solutions of the Rhodamine 6G and dye samples with identical absorbance at the same excitation wavelength were assumed to absorb the same number of photons. A simple ratio of the integrated fluorescence intensities of the two solutions (recorded under identical conditions) gave the ratio of the quantum yield values.

Results and Discussion

Compound selection and synthesis. Virtual database with 1500 molecules was created based on the chemical diversity of the styrylpyridinium dyes (Fig. 1) using MarvinSketch (MarvinSketch, ver. 14.12.15.0, 2014, ChemAxon, http://www.chemaxon.com).

To create the virtual model, the studied dyes were divided according to the intensity of their fluorescent response to the presence of fibrillar ASN I^f/I^n, where (I^n) is emission intensity of the dyes in the presence of native and (I^f) fibrillar protein. To get the prediction of the quantitative I^f/I^n ratio for new virtual compounds the regression analysis was performed for each of them.

The set of 120 dye candidates was selected for the synthesis from database by the ANN model. Based on results of the regression analysis and with consideration of chemical feasibility the series of 9 styrylpyridines containing variation of the terminal substituents were synthesized (Table. 1).

The synthesis of target dyes was carried out by the condensation of 1, 4-dimethylpyridin-1-ium iodide with benzaldehydes (Fig. 2). Diversity of the dye structures was provided by the variation of substituents in 4-position of the benzene aromatics. Required aldehydes were obtained by treatment of p-fluorobenzaldehyde with secondary amines in the presence of the base. All compounds were obtained with similar yields, with exceptions of **IId** and **IIf** dyes. The presence of the chiral center in both molecules caused lower yield at the crystallization step.

Six dyes of the selection series have close volumes and planar sizes of the molecules, while three dyes (**IIg**, **IIj**, **IIh**) are characterized by a larger size due to the aromatic substituents in 4 positions.

Fluorescent properties of dyes in a free state and in the presence of native and fibrillar insulin. The fluorescent properties of the 4-(4-dialkylaminostyryl)-pyridinium dyes in the free state, in the presence of native insulin or its fibrillar aggregates are presented in Table 2. For free dyes **IIa, IIc-IIh** the excitation maxima are located in the range 400–420 nm, while maximum of **IIb** is red shifted to

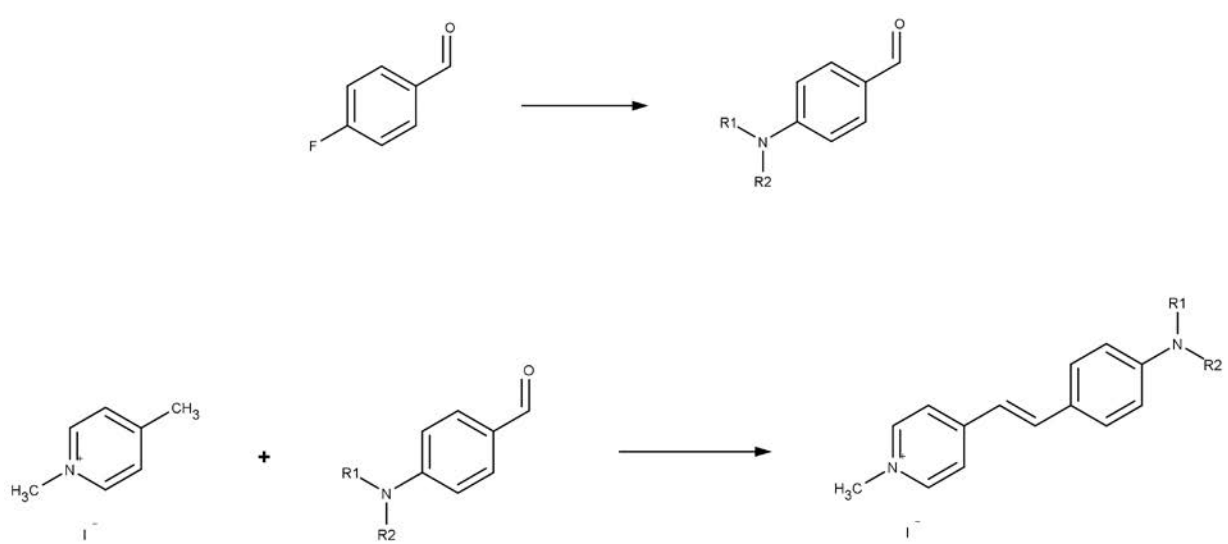

Fig. 2. General approach to the synthesis of styrylpyridines. The R1NR2 substituents are described in the Table 1.

Table 2. **The fluorescent properties of 4-(4-dialkylaminostyryl)-pyridinium dyes in free state; native insulin or fibrillar insulin aggregate presence.**

Dye	Free dye			Dye + native insulin [n]		Dye + fibrillar insulin [f]				I^f/I^n exp.	I^f/I^n pred.
	λ^{ex}, nm	λ^{em}, nm	I^n, a.u.	λ^{em}, nm	I^m, a.u.	λ^{ex}, nm	λ^{em}, nm	ΔS	I^f, a.u.		
IIa	410	616	3.9	617	3.6	533	607	74	73.0	20.3	24
IIb	477	614	7.1	611	6.7	546	606	60	88.0	13.1	17
IIc	404	605	5.6	604	4.8	498	590	92	89.0	18.5	20
IId	416	615	3.0	614	2.9	514	604	90	66.0	22.8	19
IIe	400	590	16.4	590	16.3	474	584	110	43.6	2.7	14
IIf	420	615	3.6	616	3.7	520	607	87	36.0	9.7	8
IIg	408	603	14.7	605	14.1	496	598	102	52.9	3.8	22
IIj	402	597	2.9	598	2.8	478	588	110	9.6	3.4	34
IIh	414	609	4.0	607	4.1	515	609	94	48.0	11.7	26

λ^{ex}, λ^{em} - maxima of fluorescence excitation and emission spectra;
I^n- emission intensity of dye; I^f/I^n- increase in emission of the dye in the presence of native [n] and fibrillar [f] insulin.

477 nm. The emission maxima of dyes are in the range 590–616 nm. Thus, the dyes possess a wide range of values of Stokes shift (137–206 nm). The dyes show a weak intrinsic fluorescence with the intensity in the range 2.9–16.4 a.u., the most intensive emission is observed for dyes **IIe** and **IIj** 16.4 and 14.7 a.u., respectively.

In the presence of native insulin the excitation/ emission maxima of dyes remained unchanged or slightly shifted (up to 6 nm), relatively to those of free dyes. The fluorescent properties of the dyes poorly change in the presence of native insulin that points to the weak interactions between the dyes and protein.

In the presence of fibrillar insulin the excitation maxima of dyes strongly shift to the] long-wave region (for 69–123 nm) relatively to those of the free dyes, whereas the emission maxima of the dyes slightly (up to 15 nm) shift to the short-wave region. Thus, the values of the Stokes shifts for the dyes in complexes with the fibrillar aggregates decrease comparing to those of the free dyes, however they remain quite significant (60–110 nm) (Fig. 3).

Each of the dyes give fluorescent response to the fibrillar insulin aggregates: from 2.7 times for **IIe** dye to 22.8 times for **IId** dye. The **IIa** and **IId** dyes with piperidinyl- and 4-methylpiperidinyl groups demonstrate the highest increase in the emission value (I^f/I^n) due to fibrillar insulin presence 20.3 and 22.8 times, respectively. The **IIe, IIg, IIj** dyes give a low fluorescence response (2.7 – 3.8 times) however possess the largest Stokes shifts (102–110 nm). The fluorescence quantum yields in the presence of the insulin fibrils are estimated as 4.6% and 3.7% for **IId** and **IIa** dyes, respectively.

Detection range of IIa and IId dyes for fibrillar insulin aggregates. The detection range of the fibrillar insulin was determined for two of dyes that give

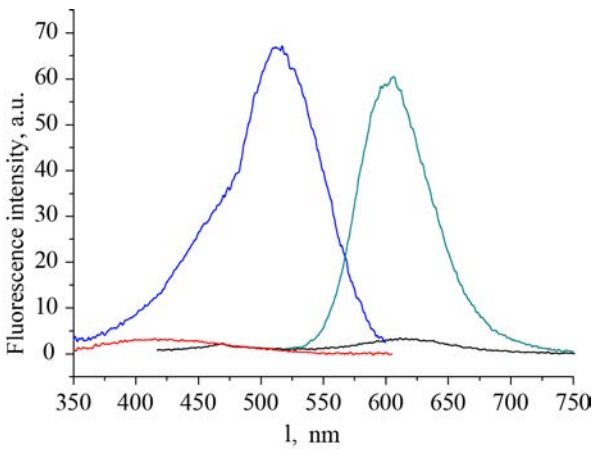

Fig. 3. Fluorescence excitation and emission spectra of the dye IId in the absence (red dash and blue dot lines) and presence of fibrillar insulin (black solid and green dash dot lines).

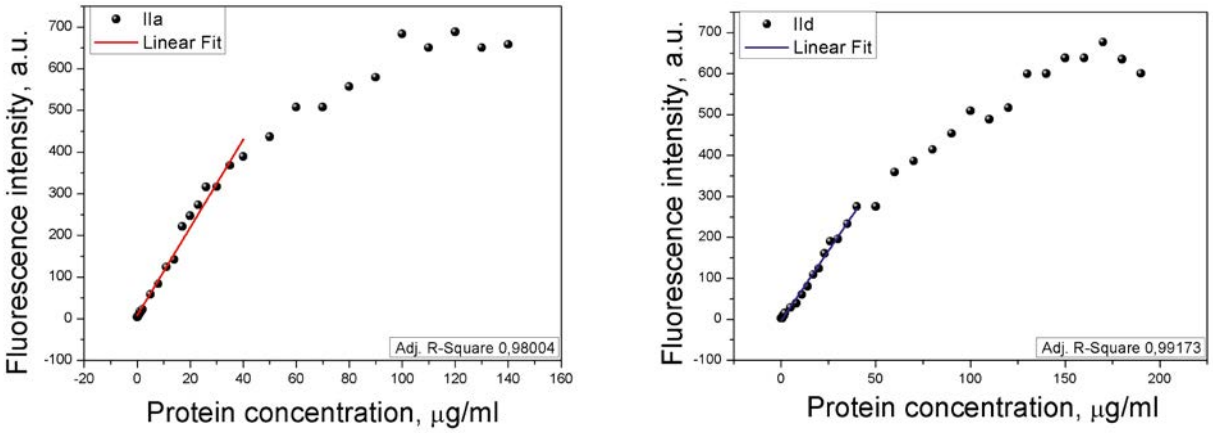

Fig. 4. Titration of dyes IIa (left) and IId (right) by fibrillar insulin. The 2 μM dye solution was used.

strong fluorescent response — **IIa** and **IIb**. For this, we performed the titration of 2 μM dyes solutions with increasing concentration of the aggregated insulin (Fig. 4). The lower limit for detecting fibrillar insulin by the dyes was determined as equal to the insulin concentration leading to a two-fold increase in fluorescence intensity. The upper limit of the detection range was estimated as the highest concentration where the dependence of the dye fluorescence intensity on the fibrils is still linear. Thus, 2 μM concentration of the dyes **IIa** and **IId** allowed the fluorescent detection of the fibrillar insulin in the linear concentration range of 0.8–40 μg/ml and 1–0 μg/ml , respectively, (Fig. 4).

This linear detection range is comparable with sensitivity of commonly used dye Thioflavin T possessing linear detection range 0.5–25 μg/ml of insulin fibrils [7].

Prediction accuracy. The predicted values of the fluorescence response ratio (I^f/I^n pred.) are presented in Table 2; comparison of this value with I^f/I^n exp. allows us to estimate the prediction accuracy of the regression model. Graphical representations of this characteristic are present in Fig. 5.

Among descriptors used in the ANN model the ovality index is one of the most valuable for the prediction of fluorescent response of the dye [9]. Ovality index is a descriptor that represents departure of the molecule from the spherical shape. It equals to 1 for the spherical molecules and increases for the longer ones [14].

The impact of ovality is associated with the mode of dye binding to the fibril – the dye molecule is suggested to locate in the groove formed by the beta-sheets parallel to the long axis of the fibril. This mode proposed for Thioflavin T binding to the amyloid fibrils is based on the dye optimal molecular dimensions (15.2 A˚ X-axis, 6.1 A˚ Y-axis and 4.3 A˚ Z-axis) [15]. For cyanine dyes the favorable parameters of molecules fluorescently sensitive to the ASN fibrils were determined to be about 3 A˚ Z-axis and up to 6.5 A˚ Y-axis that is complementary to the width and depth of the fibril binding channel. [6]. Thus, dyes with a higher ovality index (an elongated shape) fit better to the fibrillar groove and thus more tightly fixed in it.

The good prediction accuracy was observed for the styrylcyanine dyes containing unsubstituted pi-

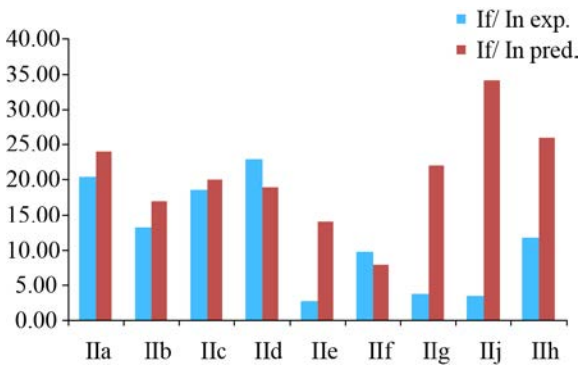

Fig. 5. Correspondence between the values of emission enhancement predicted by the model and obtained experimentally.

peridinyl, 3- and 4-substituted piperidinyl, morpholinyl, azepanyl and 4-substituted piperazinyl groups (Fig. 5).

The dyes **IIg-IIh** containing bulky groups at the 4th position (substituted with aromatics) give a noticeably lower fluorescence response than the dyes with the non-substituted or Me-substituted cyclic aliphatic group. For the molecules with aromatic groups poor prediction accuracy is observed. It could be partially related to the peculiarities of the morphology of insulin protofilaments. The B-chain of insulin forms the core of the fibrils, while the A-chain is suggested to be located outside the main fibril core [11, 16]. This way the A- chain could distort shape of the groove and hinder a tight binding of molecules with bulky groups.

The molecules containing piperazinyl fragment demonstrate poor I^f/I^n exp. ratio in comparison with their piperidine analogues (pairs **IIe** – **IId** and **IIj** – **IIh**, compound **IIg**). The piperazine cycle containing an additional aliphatic nitrogen atom possess[es] a high tendency to proton accepting (i.e. H-bonding). We suggest that due to this the tertiary aliphatic nitrogen could play a role of "anchor" – it could bind to the electron donor substituents of amino acids side groups or to the amide bonds. This way the layout of the dye molecule in the binding channel is displaced from the near-planar-planar position (Fig. 6). In this case the fixation of the dye molecule is less tight; thereby it allows additional degrees of vibrational freedom for the dye molecule and this leads to a decrease in the fluorescence response intensity [6].

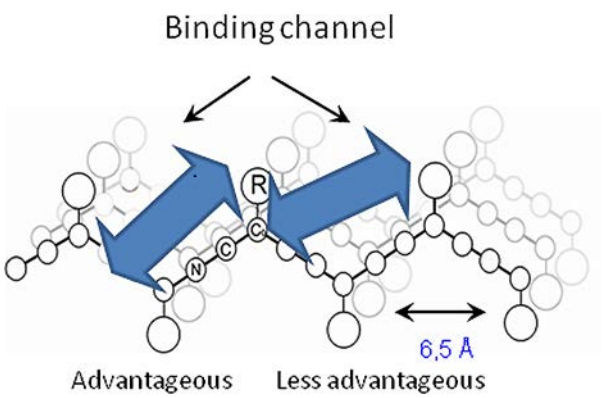

Fig. 6. Proposed schemes of the layout of styrylcyanine dye molecules into the groove of amyloid fibril. Left arrow - direct "tight" placing into the fibril groove, right - due to the interaction of the terminal nitrogen with the electron donor groups of the amino acid side chains the molecule is partially lifted out of the groove and thus less tightly fit to it.

As shown, regression model gives good prediction accuracy only for dyes with non-substituted or Me-substituted cyclic aliphatic groups **IIa-IId**, **IIf**. For the dyes **IIe**, **IIg-IIh** containing bulky aromatic substituent in cyclic aliphatic groups and/or containing piperazinyl groups the prediction accuracy is low. It points to the limitations of applicability of the earlier developed regression model and causes an interest in its further modification to provide a higher prediction accuracy.

Conclusion

The earlier developed regression model was applied for the design of dyes with fluorescence sensitivity to the amyloid fibrils. Nine styrylpiridines dyes with predicted high activity have been selected from the virtual database, synthesized and characterized for their spectral-luminescent properties.

The dyes are low fluorescent when free and insensitive to native insulin. However, they increase the emission in the presence of the insulin fibrils that is mostly pronounced for the derivatives with azepanyl, morpholinyl and 4-methylpiperidinyl terminal groups (up to 23 times).

The quantum yield of the dyes in complexes with the fibrilar protein reaches 4.6% (dye IId with 4-methylpiperidinyl group). The compounds with 4-methylpiperidinyl and piperidinyl groups possess a good linear detection range of the insulin fibrils (1–40 mkg/ml).

The regression model has shown good prediction accuracy for the dyes with non-substituted or Me-substituted cyclic aliphatic terminal groups and poor for those containing piperazinyl terminal group or bulky aromatic substituents in cyclic aliphatic groups. It points to the limitations of the prediction ability of the model.

The 4-(4-dialkylaminostyryl)-pyridinium dyes with cyclic aromatic terminal groups are proposed as prospective fluorescent molecules for sensing the amyloid aggregates of proteins.

REFERENCES

1. *Agorogiannis EI, Agorogiannis GI, Papadimitriou A, Hadjigeorgiou GM.* Protein misfolding in neurodegenerative diseases. *Neuropathol Appl Neurobiol.* 2004;**30**(3):215–24.
2. *Cohen FE, Kelly JW.* Therapeutic approaches to protein-misfolding diseases. *Nature.* 2003;**426**(6968):905–9.
3. *Raychaudhuri S, Dey S, Bhattacharyya NP, Mukhopadhyay D.* The role of intrinsically unstructured proteins in neurodegenerative diseases. *PLoS One.* 2009;**4**(5):e5566.
4. *Uversky VN, Gillespie JR, Fink AL.* Why are "natively unfolded" proteins unstructured under physiologic conditions? Proteins. *2000;41(3):415–27.*
5. *Groenning M.* Binding mode of Thioflavin T and other molecular probes in the context of amyloid fibrils-current status. *J Chem Biol.* 2010;**3**(1):1–18.
6. *Volkova KD, Kovalska VB, Balanda AO, Losytskyy MY, Golub AG, Vermeij RJ, Subramaniam V, Tolmachev OI, Yarmoluk SM.* Specific fluorescent detection of fibrillar alpha-synuclein using mono- and trimethine cyanine dyes. *Bioorg Med Chem.* 2008;**16**(3):1452–9.
7. *Kuperman MV, Chernii SV, Losytskyy MY, Kryvorotenko DV, Derevyanko NO, Slominskii YL, Kovalska VB, Yarmoluk SM.* Trimethine cyanine dyes as fluorescent probes for amyloid fibrils: The effect of N,N'-substituents. *Anal Biochem.* 2015;**484**:9–17.
8. *Kovalska V, Chernii S, Losytskyy M, Dovbii Y, Tretyakova I, Czerwieniec R, Chernii V, Yarmoluk S, Volkov S.* β-ketoenole dyes: Synthesis and study as fluorescent sensors for protein amyloid aggregates. *Dyes Pigm.* 2016; **132**:274–81.
9. *Inshyn DI, Kovalska VB, Losytskyy MY, Slominskii Y, Tolmachev OI, Yarmoluk SM.* Development of a quantitative structure activity relations (QSAR) model to guide the design of fluorescent dyes for detecting amyloid fibrils. *Biotech Histochem.* 2014;**89**(1):1–7.
10. *Haugland RP.* The handbook: a guide to fluorescent probes and labeling technologies. *10th ed.* Invitrogen Corp. 2005; 1126 p.
11. *Ivanova MI, Sievers SA, Sawaya MR, Wall JS, Eisenberg D.* Molecular basis for insulin fibril assembly. *Proc Natl Acad Sci U S A.* 2009;**106**(45):18990–5.
12. *Kubin RF, Fletcher AN.* Fluorescence quantum yields of some rhodamine dyes. *J Lumin.* 1982;**27**(4):455–62.
13. *Williams ATR, Winfield SA, Miller JN.* Relative fluorescence quantum yields using a computer controlled luminescence spectrometer. *Analyst.* 1983; **108**(1290):1067–71.
14. *Todeschini R, Consonni V.* Handbook of molecular descriptors. *WILEY-VCH, 2000, 392 p.*
15. *Krebs MR, Bromley EH, Donald AM.* The binding of thioflavin-T to amyloid fibrils: localisation and implications. *J Struct Biol.* 2005;**149**(1):30–7.
16. *Ivanova MI, Thompson MJ, Eisenberg D.* A systematic screen of beta(2)-microglobulin and insulin for amyloid-like segments. *Proc Natl Acad Sci U S A.* 2006;**103**(11):4079–82.

Дизайн (4-(4-диалкіламіностирил)–піридинових барвників для флуоресцентної детекції амілоїдних фібрил

Д. І. Іньшин, С. В. Черній, В. Б. Ковальська, С. М. Ярмолюк

Патологічна агрегація білків у бета-складчасті фібрилярні структури пов'язана з великою групою важких захворювань, серед яких нейродегенеративні розлади. У зв'язку з цим актуальною є розробка аналітичних інструментів, зокрема, флуоресцентних зондів, що дозволяють детектувати амілоїдні фібрили. **Мета.** Метою представленої роботи є дизайн амілоїдчутливих стирилпіридинових флуоресцентних барвників. **Методи.** Метод QSAR для передбачення чутливості барвників до амілоїдних фібрил, хімічних синтез, спектральні дослідження . **Результати.** Із віртуальної бази на 1500 стирилціанінів були обрані дев'ять структур із найвищою передбаченою ефективністю. Обрані сполуки були синтезовані, їх спектрально-люмінесцентні властивості були вивчені у присутності амілоїдогенного білка інсуліну. Ці барвники мають низьку власну флуоресценцію та низьку чутливість до мономерного інсуліну. У присутності фібрилярного інсуліну вони можуть збільшувати інтенсивність флуоресценції до десятків разів залежно від природи кінцевого замісника в молекулі барвника. Барвник із 4-метилпіридиновим замісником має найвищу флуоресцентну відповідь (до 23 разів) і широкий діапазон детекції амілоїд них фібрил (1-40 мкг / мл). **Висновки.** (4-(4- диалкіламіностирил) -піридинові барвники з циклічними аліфатичними кінцевими замісниками демонструють перспективні властивості як флуоресцентні зонди для детекції амілоїдних фібрил. Регресійна модель показала хорошу точність передбачення для більшості барвників, виключенням є стирилціаніни, що містять піперазиніловий та інші ароматичні замісники.

Ключові слова: флуоресценті зонди, стирилціанінові барвники, синтез, регресійна модель QSAR, амілоїдні фібрили, детекція білка

Дизайн (4-(4-диалкиламиностирил)–пиридиновых красителей для флуоресцентной детекции амилоидных фибрилл

Д. И. Иньшин, С. В. Черний, В. Б. Ковальская, С. Н. Ярмолюк

Патологическая агрегация белков в бета-складчатые фибриллярные структуры связана с большой группой тяжелых заболеваний, в частности, нейродегенеративных расстройств. В связи с этим актуальной является разработка аналитических ин-

струментов, к примеру, флуоресцентных зондов, позволяющих детектировать амилоидные фибриллы. **Цель. Целью** представленной работы является дизайн амилоид-чувствительных стирилпиридиновых флуоресцентных красителей. **Методы.** Метод QSAR для предсказания чувствительности красителя к фибриллам, синтез, спектральные исследования. **Результаты.** Из виртуальной базы на 1500 стирилцианинов были выбраны девять структур с высокой прогнозированной эффективностью. Эти соединения были синтезированы, их спектрально-люминесцентные свойства были изучены в присутствии амилоидогенного белка инсулина. Красители показали низкую собственную флуоресценцию и низкую чувствительность к мономерному инсулину. В присутствии фибриллярного инсулина они могут увеличивать интенсивность флуоресценции до десятков раз в зависимости от природы концевого заместителя в молекуле красителя. Краситель с 4-метилпиридиновым заместителем дает самый высокий флуоресцентный ответ (до 23 раз) и широкий диапазон детекции амилоидных фибрил (1-40 мкг / мл). **Выводы.** (4-(4-диалкиламиностирил)-пиридиновые красители с циклическими алифатическими конечными заместителями демонстрируют перспективные свойства как флуоресцентные зонды для детекции амилоидных фибрилл. Регрессионная модель показала хорошую точность предсказания для большинства стирилцианинов, за исключением красителей содержащих пиперазиниловий и другие ароматические заместители.

Ключевые слова: Флуоресцентные зонды, стирилцианиновые красители, синтез, регрессионная модель QSAR, амилоидные фибриллы, детекция белка

Received 20.04.2016